Volume: 8 Issues: 55 Special Issue [August, 2023] pp. 164 - 170
Journal of Islamic, Social, Economics and Development (JISED)
eISSN: 0128-1755
Journal website: www.jised.com
DOI: 10.55573/JISED.085515

IDENTIFICATION OF DETECTABLE AREA BY APPLYING INVERSE PROBLEM

Touil Dalal Radia [1]*
Lahrech Ahmed Chaouki [2]
Helifa Bachir [3]
Lefkaier Ibn Khaldoun [4]

[1] LPM Laboratory,University of Amar Telidji, Algeria, Laghouat, d.touil@lagh-univ.dz
[2] LPM Laboratory,University of Amar Telidji Algeria, Laghouat ,lahrechch@gmail.com
[3] LPM Laboratory, University of Amar Telidji,Algeria, Laghouat, helifa@yahoo.fr
[4] LPM Laboratory, University of Amar Telidji, Algeria, Laghouat, lefkaierk@gmail.com

Article history
Received date : 11-6-2023
Revised date : 12-6-2023
Accepted date : 25-7-2023
Published date : 15-8-2023

To cite this document:
Dalal Radia, T., Ahmed Chaouki, L., Bachir, H., & Ibn Khaldoun, L. (2023). Identification of detectable area by applying inverse problem. *Journal of Islamic, Social, Economics and Development (JISED)*, 8 (55), 164 – 170.

Abstract: *This work introduces the notion of the GMR sensor's effective area (EA) after being calculated and optimized using the inverse problem (Particle Swarm Optimization method (PSO)).The inverse problem goal function is minimized using (PSO) algorithm to evaluate the detectable area dimensions according to the measurement of the magnetic field strength at the GMR sensor's location. The operation of the GMR sensor is validated using 3D Finite Element experimental measurements. The prototype of the GMR sensor is developed and tested.*

Keywords: *GMR sensor, direct finite element model (FEM), inverse problem, effective area (EA), Particle Swarm Optimization method (PSO).*

Volume: 8 Issues: 55 Special Issue [August, 2023] pp. 164 - 170
Journal of Islamic, Social, Economics and Development (JISED)
eISSN: 0128-1755
Journal website: www.jised.com
DOI: 10.55573/JISED.085515

Introduction

The industry currently establishes several types of sensors used in EC-NDT. The most common eddy current probes are inductive sensors (Helifa et al., 2006; Moulder et al., 1992;Vacher., 2007), fluxgates , magneto-impedances, Hall effect sensors, and magnetoresistance sensors (Baibich et al., 1988; Hamia et al., 2013; Jander et al., 2005) EC-NDT methods have enhanced their effectiveness and efficiency through better sensor technologies, improved electronics and instrumentation, and robotic accessories. Advances in magnetic sensor technology are prompting researchers to investigate their capabilities on EC-NDTs. EC-NDT techniques can be fully explored with the emergence of these new sensors to detect small defects than before and characterize them geometrically (Postolache et al., 2011).

Nevertheless, low-frequency eddy currents (ECT) controls require sensors with high field sensitivity and spatial resolution (Hamia et al., 2010). To exceed the performance of wire wound sensors in terms of sensitivity and resolution, we use giant magnetoresistance (GMR)(Bernieri et al., 2019; Rifai et al., 2016), characterized by high sensitivity at low frequency and wide dynamic range. We are relatively easy to perform and inexpensive(Dogaru & Smith, 2001; Zorni, n.d.), which is suitable for many practical applications, including crack assessment(Rifai et al., 2016; Smith, 2004). GMR sensors in the NDT field have triggered the development of very sensitive probes (Dogaru & Smith, 2001; Gao et al., 2018). Nevertheless, GMR sensors for NDT applications are still under development; the development of magnetic sensors has made the use of low-frequency excitation fields possible and increased the method's sensitivity (Smith & Schneider, n.d.).

GMR sensors in the NDT field sparked the development of extremely sensitive probes (Gao et al., 2018). For instance, researchers like E. Ramrez-Pacheco (Ramirez-Pacheco et al., 2010) created an experimental eddy current (EC) system to identify near-side cracks in aluminum by adjusting the GMR sensor's position concerning the excitation coil's center. Romero-Arismendi in(Romero-Arismendi et al., 2020).

Initially, we assessed the area of activity of the commercial GMR sensor by utilizing the inverse problem technique that minimizes the discrepancy between the measured and computed magnetic field intensity via the application of the particle swarm optimization (PSO) algorithm.

To confirm the functionality of the GMR sensor, we conducted two types of analyses: a 3D Finite Element Model (FEM) based on the AV formulation, and experimental measurements.

Identification of detectable area by applying Inverse problem to the GMR sensor

Experimental Steps

This section proposes a simple approach to evaluate the detectable area dimensions of the GMR sensor using the inverse problem method. The proposed magnetic field measurement method is direct (the GMR sensor acts as a magnetometer by measuring the magnetic field generated by the permanent magnet). Thus, the magnetic field changes the output voltage on the GMR sensor. Figure 1 illustrates the geometric and characteristic dimensions of the numerical model implemented for magnetic field strength calculations of the permanent magnet as a distance function (Axial Magnet). There are two principal parameters of GMR sensor detectable area. The width and the height of the section. The inverse problem goal function is minimized using the particle swarm optimization (PSO) algorithm to evaluate the detectable area dimensions according to the measurement of the magnetic field strength at the GMR sensor’s location.

Volume: 8 Issues: 55 Special Issue [August, 2023] pp. 164 - 170
Journal of Islamic, Social, Economics and Development (JISED)
eISSN: 0128-1755
Journal website: www.jised.com
DOI: 10.55573/JISED.085515

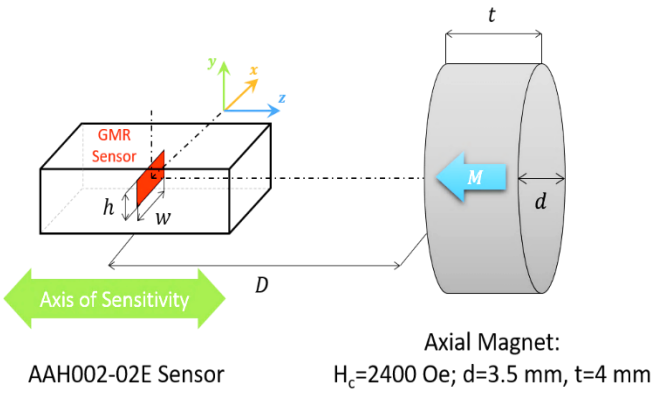

Figure 1: Geometric model representing the parameters of the numerical model implemented for magnetic field strength calculations of permanent magnet as a function of distance (Axial Magnet).

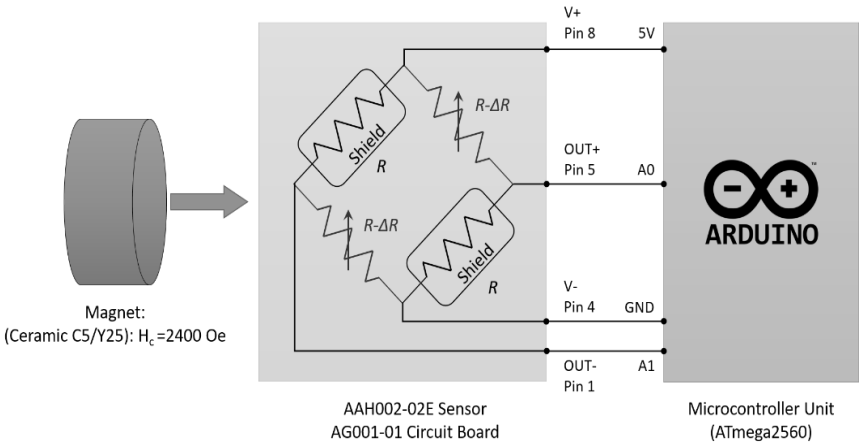

Figure 2: Schematic diagram of the experimental setup for magnetic field measurement using GMR sensor.

Simulation steps

A three-dimensional finite element model is used to understand the physical principle and study the performance of the GMR sensor. The model is based on magnetic vector potential *A* formulation, such as: *B=curl (A)* The equation solved by the finite element method in a Magneto Static application is written:

$$curl\left(\nu_0\left[\nu_r\right]curl\left(\vec{A}\right)-\vec{H}_c\right)=\vec{0} \quad (1)$$

Where the tensor of the medium's relative reluctivity is $[\upsilon_r]$, υ_0 is the magnetic reluctivity of the vacuum, $\vec{A}$ is the magnetic vector potential, and $\vec{H}_c$ is the coercive magnetic field (permanent magnets). Once the magnetic vector potential $\vec{A}$ is determined, the ''amount'' of magnetic field ''flowing'' through the surface of the GMR sensor is expressed as given by the equation (2):

$$B=\frac{\Phi_B}{S}=\frac{1}{S}\iint_s\nabla\times\left(\vec{A}\right)\circ\hat{n}da \quad (2)$$

Where $\vec{A}$ is the magnetic vector potential, *S* is the area of the surface, $\hat{n}$ is the unit vector normal to the surface, and da is a tiny area element. In the linear region of the sensor's response, we can express the output voltage as:

Volume: 8 Issues: 55 Special Issue [August, 2023] pp. 164 - 170
Journal of Islamic, Social, Economics and Development (JISED)
eISSN: 0128-1755
Journal website: www.jised.com
DOI: 10.55573/JISED.085515

$$\Delta U = S_{eff} \cdot B \tag{3}$$

S_{eff} is the adequate sensitivity that depends on the sensor type and supply voltage.

The magnetic field strength of the permanent magnet is measured using an experimental setup (Fig.2) based on a direct microcontroller interface. The magnetic field strength of the permanent magnet is calculated using a 3-D FEM model and then compared with that measured until the convergence criterion of the cost function is satisfied, as represented in (4). The detectable area dimensions of the GMR sensor are then identified. The inverse problem algorithm (Fig.4) describes these steps.

A particle swarm optimization algorithm is applied to minimize the inverse problem goal function to identify the detectable area dimensions of the GMR sensor. This algorithm is a heuristic search technique that optimizes a problem by iteratively trying to improve candidate solutions concerning a given objective measure of fitness. The inverse problem goal function is written as:

$$\cos t = \frac{1}{2}\left(\frac{B_{mes} - B_{cal}}{B_{mes}}\right) \tag{4}$$

Where B_{mes} and B_{cal}, respectively, are the permanent magnet's measured, computed magnetic field strength. The optimal detectable area dimensions of the GMR sensor, using the inverse problem method at a distance value of 18mm from the face of the magnet to the center of the AAH002-02E sensor package, are w = 0.45mm and h = 0.1mm. These values of detectable area dimensions of the GMR sensor are introduced in the 3-D model to compute the magnetic field strength of the permanent magnet as a distance function.

For an AAH002-02E GMR-based sensor S_m=145 (mV/V/mT). At a supply voltage V_s=5 (V), one obtains S_{eff}=725(mV/mT) and an estimated output voltage ΔU_α=210.25(mV) if D=18 mm.

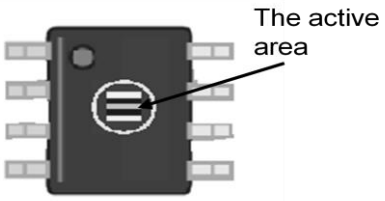

Figure 3: Position of the active area in the magnetometer proposed. (www.nve.com /catalog /accessed 04 January 2021)

Volume: 8 Issues: 55 Special Issue [August, 2023] pp. 164 - 170
Journal of Islamic, Social, Economics and Development (JISED)
eISSN: 0128-1755
Journal website: www.jised.com
DOI: 10.55573/JISED.085515

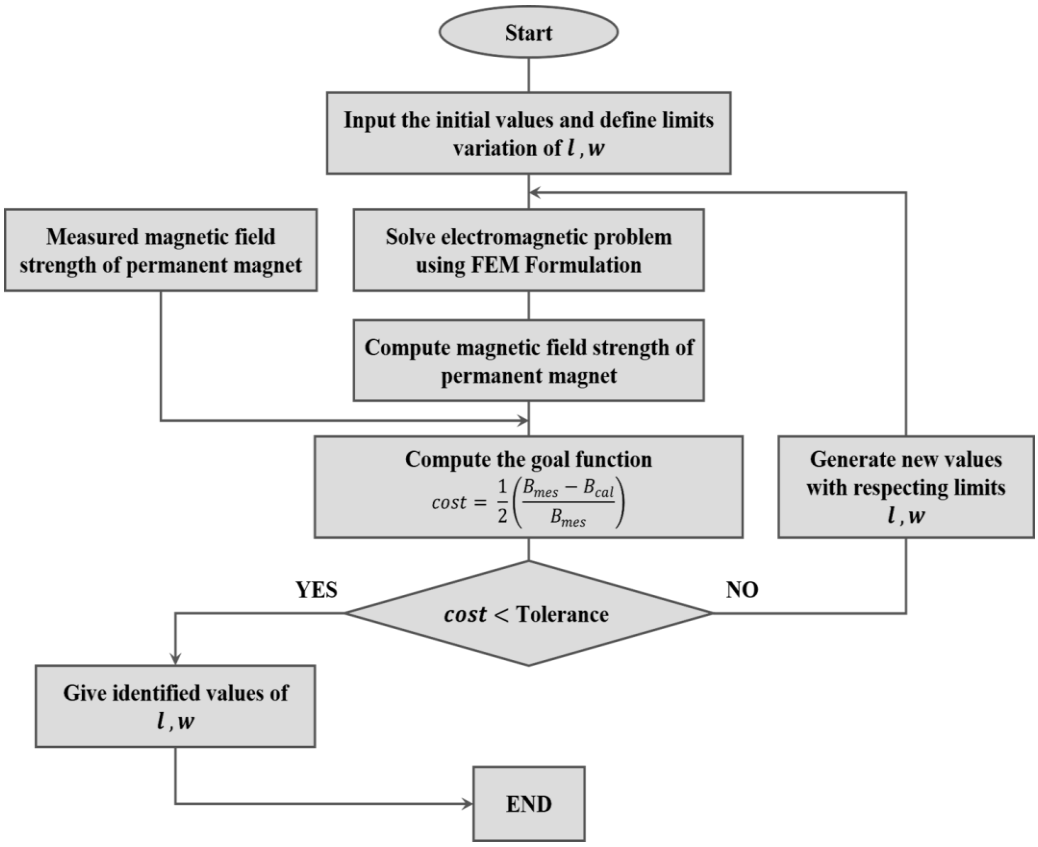

Figure 4: Inverse problem algorithm.

The inverse problem method was used to determine the ideal dimensions of the detectable area for the GMR sensor. The sensor places at a distance of 18mm from the magnet's face to the center of the AAH002-02E sensor package, as shown in Figure 3. The results of the analysis showed that the optimal dimensions for the detectable area are w = 0.45 mm and h = 0.1 mm.

Table 1: Numerical Values of the Modeled System

Element	Parameters	Values
GMR sensor	NVE AAH002-02	
	Distance between the GMR sensors (Dg)	5.34 mm
	Typical Sensitivity	150 mV/V/mT
	Linear Range	0.06 – 0.3 mT
	Saturation	0.6 mT
	Package	SOIC8

In Figure 5, a comparison presents between the 3-D computed magnetic field strength of the permanent magnet and the corresponding measured values. The experimental results confirm the accuracy of the simulation.

Volume: 8 Issues: 55 Special Issue [August, 2023] pp. 164 - 170
Journal of Islamic, Social, Economics and Development (JISED)
eISSN: 0128-1755
Journal website: www.jised.com
DOI: 10.55573/JISED.085515

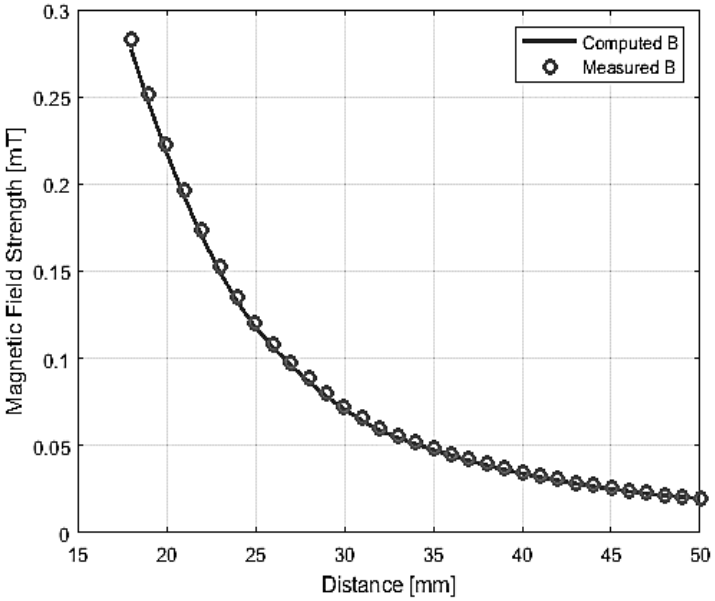

Figure 5: 3-D computed magnetic field strength of the permanent magnet and the measured one as a function of distance to identify the detectable area dimensions of the GMR sensor.

Conclusion

The 3-D model uses to compute the magnetic field strength of the permanent magnet to evaluate detectable area dimensions of the GMR AAH002 02 sensor, an experimental prototype unit consisting of the GMR sensor proposed and the permanent magnet as a distance function (Axial Magnet), and microcontroller interface.

The comparison between the 3-D computed magnetic field strength of the permanent magnet and the measured one show a significant concordance. The maximum error between the two results is less than 2%.

For future works, we propose the following: sensor simulation of GMR, AMR, and TMR magnetic sensors to increase the detection capabilities of defects in complex materials (CFCs).

Acknowledgments

We would like to express our appreciation to all those who have contributed to the research and the Materials Physics Laboratory (LPM) of Laghouat University.

References

Baibich, M. N., Broto, J. M., Fert, A., Van Dau, F. N., Petroff, F., Etienne, P., Creuzet, G., Friederich, A., & Chazelas, J. (1988). Giant Magnetoresistance of (001)Fe/(001)Cr Magnetic Superlattices. *Physical Review Letters*, *61*(21), 2472–2475. https://doi.org/10.1103/PhysRevLett.61.2472

Bernieri, A., Ferrigno, L., Laracca, M., & Rasile, A. (2019). Eddy Current Testing Probe Based on Double-Coil Excitation and GMR Sensor. *IEEE Transactions on Instrumentation and Measurement*, *68*(5), 1533–1542. https://doi.org/10.1109/TIM.2018.2890757

www.nve.com. Available online: https://www.nve.com/Downloads/catalog.pdf (accessed 04 January, 2021).

Dogaru, T., & Smith, S. T. (2001). Giant magnetoresistance-based eddy-current sensor. *IEEE*

Volume: 8 Issues: 55 Special Issue [August, 2023] pp. 164 - 170
Journal of Islamic, Social, Economics and Development (JISED)
eISSN: 0128-1755
Journal website: www.jised.com
DOI: 10.55573/JISED.085515

Transactions on Magnetics, *37*(5), 3831–3838. https://doi.org/10.1109/20.952754

Gao, P., Wang, X., Han, D., & Zhang, Q. (2018). Eddy current testing for weld defects with different directions of excitation field of rectangular coil. *2018 4th International Conference on Control, Automation and Robotics (ICCAR)*, 486–491. https://doi.org/10.1109/ICCAR.2018.8384725

Hamia, R., Cordier, C., & Dolabdjian, C. (2013). Separability of Multiple Deep Crack Defects With an NDE Eddy Current System. *IEEE Transactions on Magnetics*, *49*(1), 124–127. https://doi.org/10.1109/TMAG.2012.2218796

Hamia, R., Cordier, C., Saez, S., & Dolabdjian, C. (2010). Eddy-Current Nondestructive Testing Using an Improved GMR Magnetometer and a Single Wire as Inducer: A FEM Performance Analysis. *IEEE Transactions on Magnetics*, *46*(10), 3731–3737. https://doi.org/10.1109/TMAG.2010.2052827

Helifa, B., Oulhadj, A., Benbelghit, A., Lefkaier, I. K., Boubenider, F., & Boutassouna, D. (2006). Detection and measurement of surface cracks in ferromagnetic materials using eddy current testing. *NDT & E International*, *39*(5), 384–390. https://doi.org/10.1016/j.ndteint.2005.11.004

Jander, A., Smith, C., & Schneider, R. (2005). *Magnetoresistive Sensors for Nondestructive Evaluation*.

Moulder, J. C., Uzal, E., & Rose, J. H. (1992). Thickness and conductivity of metallic layers from eddy current measurements. *Review of Scientific Instruments*, *63*(6), 3455–3465. https://doi.org/10.1063/1.1143749

Vacher, François. Développement d'un imageur magnétique pour le contrôle non destructif par courants de Foucault. Diss. Cachan, Ecole normale supérieure, 2007.

Postolache, O., Ramos, H. G., & Ribeiro, A. L. (2011). Detection and characterization of defects using GMR probes and artificial neural networks. *Computer Standards & Interfaces*, *33*(2), 191–200. https://doi.org/10.1016/j.csi.2010.06.011

Ramirez-Pacheco, E., Espina-Hernandez, J. H., Caleyo, F., & Hallen, J. M. (2010). Defect Detection in Aluminium with an Eddy Currents Sensor. *2010 IEEE Electronics, Robotics and Automotive Mechanics Conference*, 765–770. https://doi.org/10.1109/CERMA.2010.91

Rifai, D., Abdalla, A., Ali, K., & Razali, R. (2016). Giant Magnetoresistance Sensors: A Review on Structures and Non-Destructive Eddy Current Testing Applications. *Sensors*, *16*(3), 298. https://doi.org/10.3390/s16030298

Romero-Arismendi, N. O., Pérez-Benítez, J. A., Ramírez-Pacheco, E., & Espina-Hernández, J. H. (2020). Design method for a GMR-based eddy current sensor with optimal sensitivity. *Sensors and Actuators A: Physical*, *314*, 112348. https://doi.org/10.1016/j.sna.2020.112348

Smith, C. H. (2004). Eddy-Current Testing with GMR Magnetic Sensor Arrays. *AIP Conference Proceedings*, *700*, 406–413. https://doi.org/10.1063/1.1711651

Smith, C. H., & Schneider, R. W. (n.d.). *Low-Field Magnetic Sensing with GMR Sensors*.

Zorni, C. (n.d.). *Contrôle non destructif par courants de Foucault de milieux ferromagnétiques: De l'expérience au modèle d'interaction*.